Opposite carrier dynamics and optical absorption characteristics under external electric field in nonpolar *vs.* polar InGaN/GaN based quantum heterostructures

Emre Sari,[1] Sedat Nizamoglu,[1] Jung-Hun Choi,[2] Seung-Jae Lee,[3] Kwang-Hyeon Baik,[4] In-Hwan Lee,[2] Jong-Hyeob Baek,[3] Sung-Min Hwang[4] and Hilmi Volkan Demir[1,5,*]

[1] *Department of Electrical and Electronics Engineering, Department of Physics and UNAM – Institute of Materials Science and Nanotechnology, Bilkent University, 06800 Bilkent, Ankara, Turkey*
[2] *School of Advanced Materials Engineering, Chonbuk National University, Chonju 561-756, Korea*
[3] *Korea Photonics Technology Institute, Gwangju, 500-460 Korea*
[4] *Optoelectronics Lab., Korea Electronics Technology Institute, Seongnam, Gyeonggi 463-816, Korea*
[5] *School of Electrical and Electronic Engineering, Microelectronics Division; School of Physical and Mathematical Sciences, Physics and Applied Physics Division, Nanyang Technological University, 639798 Singapore*
**volkan@bilkent.edu.tr*

Abstract: We report on the electric field dependent carrier dynamics and optical absorption in nonpolar *a*-plane GaN-based quantum heterostructures grown on *r*-plane sapphire, which are surprisingly observed to be opposite to those polar ones of the same materials system and similar structure grown on *c*-plane. Confirmed by their time-resolved photoluminescence measurements and numerical analyses, we show that carrier lifetimes increase with increasing external electric field in nonpolar InGaN/GaN heterostructure epitaxy, whereas exactly the opposite occurs for the polar epitaxy. Moreover, we observe blue-shifting absorption spectra with increasing external electric field as a result of reversed quantum confined Stark effect in these polar structures, while we observe red-shifting absorption spectra with increasing external electric field because of standard quantum confined Stark effect in the nonpolar structures. We explain these opposite behaviors of external electric field dependence with the changing overlap of electron and hole wavefunctions in the context of Fermi's golden rule.

OCIS codes: (160.4760) Optical properties; (160.6000) Semiconductor materials; (230.0250) Optoelectronics.

References and links

1. S. Nakamura, M. Senoh, N. Iwasa, and S. Nagahama, "High power InGaN single-quantum-well-structure blue and violet light-emitting diodes," Appl. Phys. Lett. **67**(13), 1868–1870 (1995).
2. S. Nakamura, M. Senoh, S. Nagahama, N. Iwasa, T. Yamada, T. Matsushita, Y. Sugimoto, and H. Kiyoku, "Room-temperature continuous-wave operation of InGaN multi-quantum-well structure laser diodes," Appl. Phys. Lett. **69**(26), 4056–4058 (1996).
3. S. Nizamoglu, G. Zengin, and H. V. Demir, "Color-converting combinations of nanocrystal emitters for warm-white light generation with high color rendering index," Appl. Phys. Lett. **92**(3), 031102–031104 (2008).
4. H. X. Jiang, S. X. Jin, J. Li, J. Shakya, and J. Y. Lin, "III-nitride blue microdisplays," Appl. Phys. Lett. **78**(9), 1303–1305 (2001).
5. E. Sari, S. Nizamoglu, T. Ozel, and H. V. Demir, "Blue quantum electroabsorption modulators based on reversed quantum confined Stark effect with blueshift," Appl. Phys. Lett. **90**(1), 011101 (2007).
6. D. Walker, E. Monroy, P. Kung, J. Wu, M. Hamilton, F. J. Sanchez, J. Diaz, and M. Razeghi, "High-speed, low-noise metal–semiconductor–metal ultraviolet photodetectors based on GaN," Appl. Phys. Lett. **74**(5), 762 (1999).
7. J. Goldberger, R. He, Y. Zhang, S. Lee, H. Yan, H.-J. Choi, and P. Yang, "Single-crystal gallium nitride nanotubes," Nature **422**(6932), 599–602 (2003).
8. B. Monemar, and G. Pozina, ""Group III-nitride based hetero and quantum structures," Prog. Quantum Electron. **24**(6), 239–290 (2000).

#140055 - $15.00 USD Received 22 Dec 2010; revised 23 Feb 2011; accepted 25 Feb 2011; published 8 Mar 2011

9. C. Wetzel, M. Zhu, J. Senawiratne, T. Detchprohm, P. D. Persans, L. Liu, E. A. Preble, and D. Hanser, "Light-emitting diode development on polar and non-polar GaN substrates," J. Cryst. Growth **310**(17), 3987–3991 (2008).
10. T. Paskova, R. Kroeger, D. Hommel, P. P. Paskov, B. Monemar, E. Preble, A. Hanser, N. M. Williams, and M. Tutor, "Nonpolar a- and m-plane bulk GaN sliced from boules: structural and optical characteristics," Phys. Status Solidi **4**(7), 1610–1642 (2007).
11. K. Okamoto, H. Ohta, D. Nakagawa, M. Sonobe, J. Ichihara, and H. Takasu, "Dislocation-Free m-Plane InGaN/GaN Light-Emitting Diodes on m-Plane GaN Single Crystals," Jpn. J. Appl. Phys. **45**(45), L1197–L1199 (2006).
12. M. C. Schmidt, K.-C. Kim, R. M. Farrell, D. F. Feezell, D. A. Cohen, M. Saito, K. Fujito, J. S. Speck, S. P. DenBaars, and S. Nakamura, "Demonstration of Nonpolar m-Plane InGaN/GaN Laser Diodes," Jpn. J. Appl. Phys. **46**(9), L190–L191 (2007).
13. S.-M. Hwang, Y.-G. Seo, K.-H. Baik, I.-S. Cho, J.-H. Baek, S.-K. Jung, T. G. Kim, and M.-W. Cho, "Demonstration of nonpolar a-plane InGaN/GaN light emitting diode on r-plane sapphire substrate," Appl. Phys. Lett. **95**(7), 071101 (2009).
14. G. A. Garrett, H. Shen, M. Wraback, A. Tyagi, M. C. Schmidt, J. S. Speck, S. P. DenBaars, and S. Nakamura, "Comparison of time-resolved photoluminescence from InGaN single quantum wells grown on nonpolar and semipolar bulk GaN substrates," Phys. Status Solidi C **6**(S2), S800–S803 (2009).
15. M. Häberlen, T. J. Badcock, M. A. Moram, J. L. Hollander, M. J. Kappers, P. Dawson, C. J. Humphreys, and R. A. Oliver, "Low temperature photoluminescence and cathodoluminescence studies of nonpolar GaN grown using epitaxial lateral overgrowth," J. Appl. Phys. **108**(3), 033523–033529 (2010).
16. E. Lioudakis, A. Othonos, E. Dimakis, E. Iliopoulos, and A. Georgakilas, "Ultrafast carrier dynamics in $In_xGa_{1-x}N$ (0001) epilayers: Effects of high fluence excitation," Appl. Phys. Lett. **88**(12), 121128 (2006).
17. E. Sari, S. Nizamoglu, I.-H. Lee, J.-H. Baek, and H. V. Demir, "Electric field dependent radiative decay kinetics of polar InGaN/GaN quantum heterostructures at low fields," Appl. Phys. Lett. **94**(21), 211107 (2009).
18. Y. D. Jho, J. S. Yahng, E. Oh, and D. S. Kim, "Field-dependent carrier decay dynamics in strained $In_xGa_{1-x}N$/GaN quantum wells," Phys. Rev. B **66**(3), 035334 (2002).
19. Y. D. Jho, Y. S. Yahng, E. Oh, and D. S. Kim, "Measurement of piezoelectric field and tunneling times in strongly biased InGaN/GaN quantum wells," Appl. Phys. Lett. **79**(8), 1130 (2001).
20. Y. C. Shen, G. O. Mueller, S. Watanabe, N. F. Gardner, A. Munkholm, and M. R. Krames, "Auger recombination in InGaN measured by photoluminescence," Appl. Phys. Lett. **91**(14), 141101 (2007).
21. D. A. B. Miller, D. S. Chemla, T. C. Damen, A. C. Gossard, W. Wiegmann, T. H. Wood, and C. A. Burrus, "Electric field dependence of optical absorption near the band gap of quantum-well structures," Phys. Rev. B Condens. Matter **32**(2), 1043–1060 (1985).

1. Introduction

Since the first demonstration of blue light emitting diodes (LEDs) [1] and blue laser diodes (LDs) [2] in the mid-'90s, GaN based optoelectronic devices have found important industrial applications in lighting [3] and display [4] technologies. Also, since then, GaN systems have offered other promising applications [5–7]. In order to further expand their use on a wider scale, the material quality and efficiency of these devices need to be delivered at reduced costs. But, unlike GaAs and InP based systems, it is expensive and challenging to obtain a large enough native substrate to grow these III-N structures with low threading dislocation density. Presently, the most common substrate used for the growth of GaN and related alloys is sapphire, thanks to its lower mismatch of structural parameters, including lattice constant and thermal expansion coefficient, compared to other types of substrates. Specifically, the lattice mismatch of *c*-plane sapphire substrate is sufficiently low with respect to *c*-plane GaN epitaxy, which makes its epitaxial growth feasible, despite being a non-native substrate. However, such III-N quantum heterostructure epitaxy (e.g., quantum wells/barriers) exhibits high polarization-induced electrostatic fields, due to the discontinuity of their net polarization fields (i.e., the vector sum of their spontaneous and piezoelectric components) when grown in the so-called "polar" direction on *c*-plane. In such polar heterostructures, the polarization-induced electric field inside the well region pulls the bound electron and hole in opposite directions. This reduces their wavefunction overlap and in turn reduces their oscillator strength and thus their radiative recombination rate [8]. This makes the polar III-Nitrides less favorable for light generation in device applications including light emitting diodes and laser diodes. Therefore, it is highly desired to obtain GaN epitaxy on other planes of its unit cell, where there is no polarization discontinuity in quantum well structures. This is, however, technically challenging.

#140055 - $15.00 USD Received 22 Dec 2010; revised 23 Feb 2011; accepted 25 Feb 2011; published 8 Mar 2011

Such polarization-free (nonpolar) planes are *m*- and *a*-planes of the GaN's wurtzite crystal [9]. To date, many techniques have previously been proposed for obtaining high-quality nonpolar GaN crystals [10]. Also, LEDs [11] and LDs [12] have been demonstrated using these techniques. Very few of these prior works involved a feasible and efficient process, though. In a very recent work, Hwang *et al.* [13] made it possible to grow *a*-plane GaN on *r*-plane sapphire by reducing defect densities and demonstrated working light emitting diodes incorporating these nonpolar InGaN/GaN quantum structures, using metal-organic chemical vapor deposition (MOCVD) technique while avoiding the need for growing on a very thick (>10 μm) GaN template.

In the past, several physically important phenomena were investigated in polar and nonpolar epitaxial materials, e.g., through time resolved photoluminescence [14], cathodoluminescence [15] and differential transmission and reflection measurements [16]. Especially related with our current investigation, electric field dependent optical absorption [5] and time and spectrum-resolved photoluminescence [17–19] studies were performed in polar structures by our group and others. However, these analyses, which are fundamentally important for the understanding of operation and performance of various devices, have not been studied in such nonpolar GaN–based quantum heterostructures. Also, a comparative study on their characteristics between nonpolar and polar InGaN/GaN quantum heterostructure epitaxy has not been reported till date.

In our previous study, we investigated carrier lifetimes in polar InGaN/GaN quantum structures under different levels of external electric field [17]. The carrier lifetimes were then shown to decrease strongly with increasing reverse bias in these polar structures [17], also consistent with two other previous studies [18,19]. There are at least two reasons behind this observation: One of them is that the reverse bias generates electric field in the opposite direction to polarization-induced field inside the well layer, given that the growth technique is MOCVD and the device architecture is *p*-*i*-*n*, with *p*-side on the top. This increasing reverse bias directly shortens radiative component of the carrier lifetime through the increased squared-overlap-integral of electron and hole wavefunctions by Fermi's golden rule. The other reason is the dissociation of excitons through carrier drift, leading to shortened nonradiative component of the carrier lifetime. In an earlier study, we also showed that absorption spectra shift with increasing external electric field in such polar InGaN/GaN quantum heterostructures and demonstrated reversed quantum confined Stark effect [5]. The physical explanation for this phenomenon is that the energy difference between the electron and hole ground states at which the vertical transition takes place increases with the external electric field that is in the opposite direction to the built-in polarization-induced electrostatic fields inside the well layers. An in-house developed quantum mechanics modeling tool based on transfer matrix method was further used for the physical understanding and simulation of these findings.

In this paper, different than prior works of our group and others, we present a study on the field dependent carrier dynamics and optical absorption characteristics of InGaN/GaN quantum heterostructures in nonpolar crystal orientation on *a*-plane to compare against those in polar orientation on *c*-plane. In both cases, the quantum structures are housed in the intrinsic region of a *p*-*i*-*n* diode, with the *p*-region on the top. Using these comparative sets of nonpolar vs. polar quantum heterostructures, we observe surprisingly a completely opposite behavior in the external electric field dependence of their carrier lifetimes and optical absorptions in their respective reverse and forward biases in both time-resolved photoluminescence (TRPL) and steady-state photocurrent measurements and numerical analyses. Our results for the polar, *c*-plane grown devices are in agreement with the previously reported results, in which decreased carrier lifetime [17–19] and blue-shifting absorption edge [5] were observed with increasing reverse bias voltages.

2. Growth and fabrication

The quantum heterostructures studied in this work were epitaxially grown on *r*-plane and *c*-plane sapphire substrates, both using MOCVD as described elsewhere previously (e.g., see

#140055 - $15.00 USD Received 22 Dec 2010; revised 23 Feb 2011; accepted 25 Feb 2011; published 8 Mar 2011

[13] and [14], respectively). They were incorporated in a *p*-*i*-*n* diode architecture, and their *n*-type layer was on the bottom while their *p*-type layer was on the top. These epi-structures included (i) two 7 nm thick $In_{0.20}Ga_{0.80}N$ quantum wells separated by a 12 nm GaN barrier in the nonpolar case and (ii) five 2.5 nm thick $In_{0.18}Ga_{0.82}N$ quantum wells separated by 7.5 nm GaN barriers in the polar case. Although these multi-quantum well structures are slightly different, they are essentially the same type of uncoupled quantum structures, with their peak photoluminescence emission wavelengths close to each other, both exhibiting strong emission around λ~500 nm. Moreover, for both structures, the electron concentrations throughout the active (multiple quantum well) region were approximately $4x10^{17}$ cm^{-3}. Subsequent to their epitaxial growth, the devices were fabricated in a clean room environment using the same standard lithography, reactive ion etching and metal evaporation/sputtering steps. The devices were then diced and wire-bonded to metal can packages for compact and reproducible device characterization.

3. Materials and device characterization

The photoluminescence (PL) spectra of our quantum structure samples were measured using a He-Cd laser to pump at an excitation wavelength of 325 nm and a spectrometer to collect the emission signal. From these PL spectra, using Gaussian fitting procedure, (i) a peak emission wavelength at 514 nm with a full width at half maximum (FWHM) of 43.1 nm for the nonpolar heterostructure on *a*-plane and (ii) a peak wavelength of 491 nm with a FWHM of 37.5 nm for the polar heterostructure on *c*-plane were obtained. Their measured photoluminescence spectra are shown in Fig. 1.

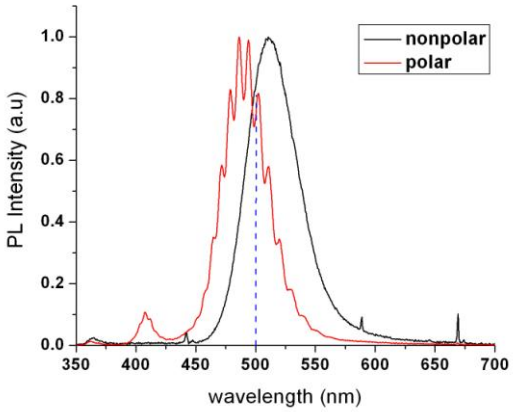

Fig. 1. Normalized photoluminescence (PL) spectra of our InGaN/GaN based polar and nonpolar quantum heterostructures at room temperature. The dashed blue line shows the TRPL emission wavelength, 500 nm.

It is clear that for both epi-structures, the presented photoluminescence originates from the quantum well structures. Moreover, both exhibit electroluminescence when their devices are forward-biased as given in Fig. 2.

#140055 - $15.00 USD Received 22 Dec 2010; revised 23 Feb 2011; accepted 25 Feb 2011; published 8 Mar 2011

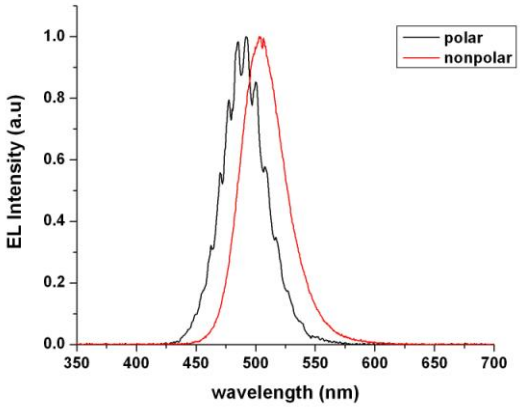

Fig. 2. Normalized electroluminescence (EL) spectra of our devices based on polar and nonpolar InGaN/GaN quantum heterostructures, both measured at a constant driving current of 20 mA at room temperature.

3.1 Electric field dependence of carrier lifetimes

The carrier lifetimes (τ) of these quantum structures were measured at room temperature using a commercially available time-resolved photoluminescence setup (from PicoQuant GmbH) that contains an InGaN/AlGaN based pump diode laser, emitting at 375 nm and operated in pulsed mode. The experimental conditions were kept the same for both devices. Average and peak intensities of laser excitation were kept at low values, at around 3 and 6 W/cm^2, respectively, to avoid band filling effect and thus evolution of higher energy states. Moreover, at such laser excitation intensity levels, with the given carrier densities in the active region, the effect of Auger recombination on the carrier lifetimes is insignificant [20]. The measurement setup also consists of a monochromator, a photomultiplier tube and controller electronics. We set the pass band center wavelength of the monochromator to 500 nm for both sets of measurements. As depicted with a straight dashed (blue) line in the PL spectra of both epi-structures (Fig. 1), 500 nm corresponds to a strong emission wavelength.

In Fig. 3, we present the photoluminescence decay time traces of the polar hetero-epitaxy on *c*-plane under different levels of external bias. As a general trend, the photoluminescence first starts to decay faster with stronger electric field as the reverse bias is increased, but then the reverse bias voltages greater than 1.00 V show a diminishing effect. Such a photoluminescence decay behavior modified with the external field application is in conformity with the observations in the previous works of our group [14] and Jho *et al*. [15,16] (for the reasons discussed in the Introduction part). In forward bias, however, the polar epi-structure's decay profile slows down as the voltage is increased to 0.25 V, and then the subsequent decay profiles exhibit an inflection point at a time delay of around 50 ns, seen as an increased time constant of the fast component but as a decrease of the overall transient behavior. The increase of fast (nonradiative) component time constant can be explained by the decreased density of the available trap states near the quantum well region, whereas the decrease of the slow (radiative) component time constant, and thus the overall lifetime, can be attributed to the increased density of electrons and holes in the same region through formation of quasi-Fermi levels. For forward and reverse bias voltages of 1.00-2.00 V, we observe no significant change in their decay profiles.

#140055 - $15.00 USD Received 22 Dec 2010; revised 23 Feb 2011; accepted 25 Feb 2011; published 8 Mar 2011

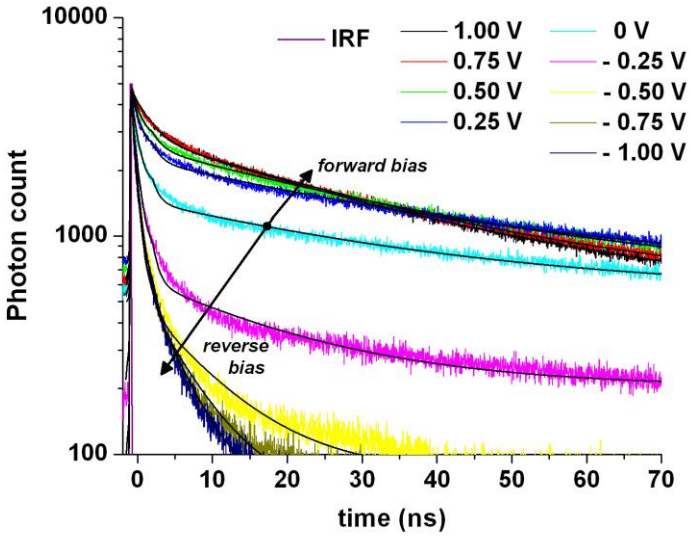

Fig. 3. Room temperature time-resolved photoluminescence (RT-TRPL) traces and numerical fits of our device with polar InGaN/GaN quantum heterostructures under different bias levels.

Similarly, Fig. 4 shows the photoluminescence decay time traces of nonpolar epitaxy on *a*-plane with respect to different levels of external electric field. For this set of epi-structure, the electric field dependence is observed to be in the opposite way, where the photoluminescence decays become slower as the external electric field is increased in reverse bias. This results from the reduced overlap integral of electron and hole wavefunctions in the initially nearly square potential well in response to an externally applied electric field. Nevertheless, with increasing reverse bias voltages, the overall time constant of nonradiative component does not decrease as much at low levels of the external electric fields. The nonpolar structure's time-resolved photoluminescence profiles also exhibit faster decays, again opposite to the polar case, as the forward bias voltage is increased (where the lifetimes were measured down to the measurement limit of our optical experimental setup). Again, at such low voltage levels of forward bias, the decreased lifetimes can be explained through compensation of built-in voltage with the external electric field and at some field level, forming an almost perfectly square potential well, which would yield the shortest lifetime.

#140055 - $15.00 USD Received 22 Dec 2010; revised 23 Feb 2011; accepted 25 Feb 2011; published 8 Mar 2011

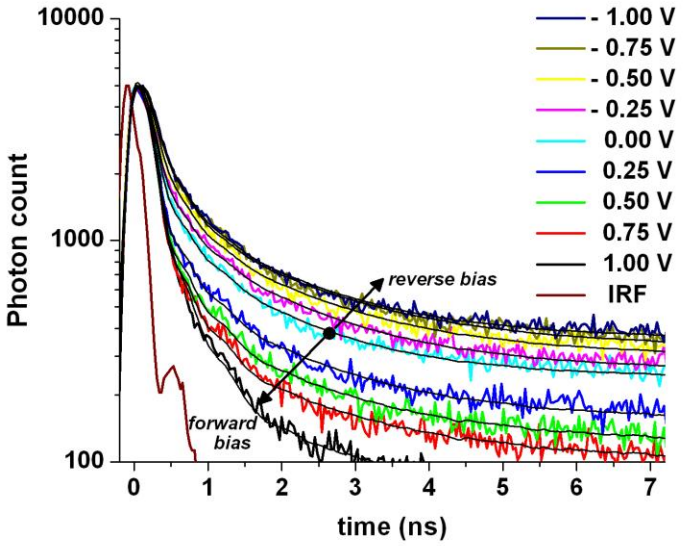

Fig. 4. Room temperature time-resolved photoluminescence (RT-TRPL) traces and numerical fits of our device with nonpolar InGaN/GaN quantum heterostructures under different bias levels.

In our time-resolved analyses, we perform de-convolution of impulse response function (IRF) from the signal and apply a biexponential numerical fitting procedure with low error (χ^2 close to unity) for all decay profiles. We then extract carrier lifetimes (τ) by averaging the time constants, τ_1 and τ_2, with their respective total intensities, i.e., their weights. Thus, the time constants we obtain in this procedure contain information on both slow and fast components of the overall decay profile. The corresponding numerical fits were provided in the decays. From these numerical analyses, we extract the carrier lifetimes as a function of external electric field for both structures as depicted in Fig. 5. These analysis results also reveal the opposite behavior in nonpolar *vs.* polar quantum heterostructures in terms of carrier lifetimes under electric field. Here, we present the lifetimes as a function of externally applied electric fields, rather than voltages, in order to make a meaningful comparison between the two sets of data. Hence, for both structures, we assume that the total voltage drop across the devices is in the depletion regions. We further assume that the depletion widths are 50 nm, and that they do not change by such low voltage application. With these approximations, we do not lose any generality for our points discussed in this paper. This opposite behavior could be qualitatively explained by quantum confined Stark effect (QCSE) and Fermi's golden rule considering the increased *vs.* decreased squared-overlap integrals of electron and hole wavefunctions (under the assumption that the nonradiative components of the decays would not change with the external electric field within the range of interest) [14,16].

#140055 - $15.00 USD Received 22 Dec 2010; revised 23 Feb 2011; accepted 25 Feb 2011; published 8 Mar 2011

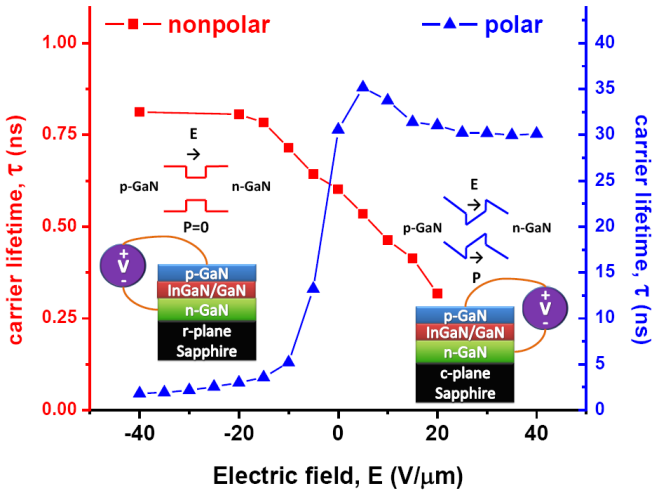

Fig. 5. Carrier lifetime (τ) vs external electric field (E) for the polar and nonpolar devices. Note that here E is taken to be positive for the forward bias and negative for the reverse bias.

3.2 Electric field dependence of optical absorption

We also comparatively investigated the external field dependent optical absorption in our polar and nonpolar InGaN/GaN based devices through photocurrent measurements. Our photocurrent setup consists of a Xenon lamp, monochromator, optical chopper, DC power supply and a lock-in amplifier. We measured the photocurrent both in our polar and nonpolar devices around the wavelength of their absorption edges at different reverse bias levels at room temperature. Here shown in a semilog plot of the photocurrent spectra in Fig. 6, the polar device exhibits a blue-shifting absorption edge with the applied field due to reversed quantum confined Stark effect.

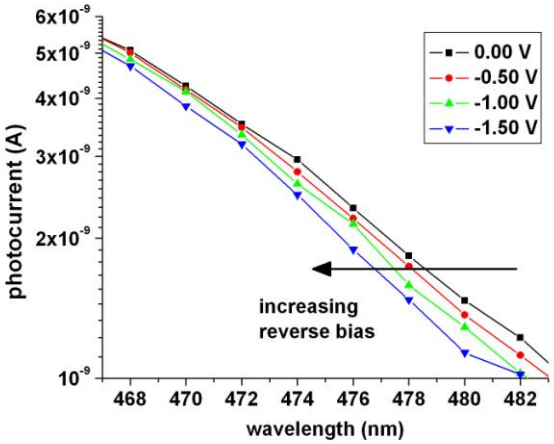

Fig. 6. Photocurrent spectra of our device based on polar InGaN/GaN quantum heterostructures. The arrow indicates the blue shift of the absorption edge with the increasing reverse bias.

In the opposite manner, for the nonpolar structure, we observe a red-shifting trend of the absorption edge, as a result of quantum confined Stark effect [21] that manifests itself as in other III-V systems such as InP/GaAs as in Fig. 7. Due to the narrower bandgap of the

#140055 - $15.00 USD Received 22 Dec 2010; revised 23 Feb 2011; accepted 25 Feb 2011; published 8 Mar 2011

quantum well material, here for the nonpolar quantum structures the absorption edge is at longer wavelengths, around λ~500 nm.

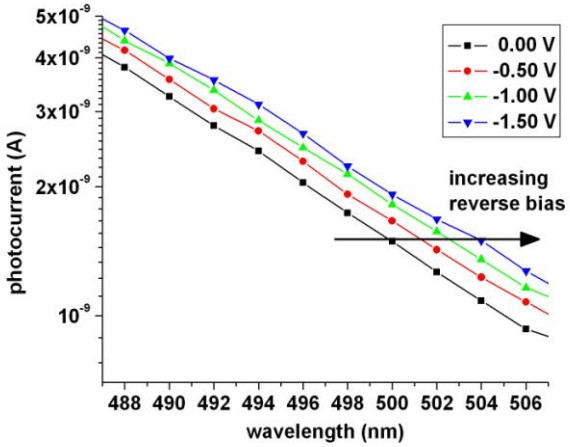

Fig. 7. Photocurrent spectra of our device based on nonpolar InGaN/GaN quantum heterostructures. The arrow indicates the red shift of the absorption edge with the increasing reverse bias.

4. Conclusion

In conclusion, we presented the opposite external electric field dependence of carrier lifetimes and optical absorption characteristics in *c*-plane grown polar *vs. a*-plane grown nonpolar InGaN/GaN quantum heterostructures. We showed using time-resolved photoluminescence measurements that carrier lifetimes decrease with increasing external electric fields in polar quantum epi-structures, whereas the opposite occurs in nonpolar quantum epi-structures. In addition, we presented the blue shift of the absorption edge in polar quantum heterostructures and the red shift of the absorption edge in nonpolar heterostructures. We explained these opposite behaviors in the context of Fermi's golden rule as well as quantum confined Stark effect.

Acknowledgments

This work is supported by EU-FP7 Nanophotonics4Energy NoE, and TUBITAK Grant Nos. EEEAG 109E002, 109E004, and 110E010. H.V.D. acknowledges support from ESF-EURYI and TUBA GEBIP, and E.S. from TUBITAK-BIDEB 2211.

#140055 - $15.00 USD Received 22 Dec 2010; revised 23 Feb 2011; accepted 25 Feb 2011; published 8 Mar 2011